

A nanocomposites photo electrode made of 2.2 eV band gap CuWO_4 and multi-wall carbon nanotubes for solar-assisted water splitting

Mr. Mahra Singh (Research Scholar), Dr. Shailesh Kumar Singh (Head of Department)
Department of Physics, Monad University, Hapur, Uttar Pradesh (India)

Abstract

We record on the photo electrochemical performances of a nanocomposites image energetic cloth made of copper tungsten (CuWO_4) and multi-wall carbon nanotubes (MWCNT). The reason of this paintings become to create a mild ABSORBED/Charge collector composite fabric with unable digital delivery properties to decrease the bulk resistance of CuWO_4 material magnificence. Nano composites skinny films (commonly 2.zero T 0.1 mm) had been fabricated by spray pyrolysis using answers containing copper acetate, ammonium metatungstate and MWCNT. Spray-deposited poly crystalline CuWO_4 movies were discovered to be porous, even though crack-free, and made of CuWO_4 nano debris with dimensions in the 10e50 nm range. Tauc plots derived from UVvisible and photo contemporary spectroscopy techniques brought about a constant band hole fee of 2.20 (T0.05) eV. Electrochemical impedance spectroscopy finished in pH10 buffer answer below Air Mass 1.5 international (AM1.5G) at 0.eight V vs. Saturated calomel electrode (1.63V vs. Reversible hydrogen electrode) pointed out a bulk resistance reduction by using 30% on nanocomposites picture anodes when in comparison to un-modified CuWO_4 manage samples. It is really worth citing that the reduction in bulk resistance changed into performed with a really low MWCNT: CuWO_4 weight ratio (1:10,000), wherein MWCNT absorbed less than 2% of incoming light. Subsequent linear scan voltammeter (LSV) executed within the equal situations found out a photograph contemporary density increase of 26% at 0.8 VSCE (1.63 VRHE) as compared to manage samples. Additional LSV and incident photon-to-cutting-edge efficiency measurements established that MWCNT served as effective electron collectors distributed throughout the entire CuWO_4 bulk.

Keywords: Photo electrochemical cell (PEC), Spray-pyrolysis, Multi-wall carbon nanotubes, CuWO_4 , Bulk resistance, Electronic transport.

Introduction

The capability to provide power from dependable, low-priced, sustainable and secure sources is crucial to address the economic and environmental demanding situations that the arena is presently going through. Among all viable thermodynamic pathways, direct sun-to-electron conversion, together with the with no trouble deployed image voltaic (PV) is taken into consideration as one of the most green routes to supply our electricity wishes. However, the region and time of PV operation require shipping and garage of generated electricity, which each incur energetic losses. Converting solar power directly into chemical energy is a realistic way to cope with each electricity garage and transport in decentralized systems, and may in precept be found out in photograph-electrochemical cells (PEC). The so-called "sun fuels" can take diverse forms (H_2 , CH_4 , and C_2H_4 .and many others.) and be transformed on call for into mechanical or electrical electricity. Several picture- electrochemical structures capable of sun-fuel production had been advanced over the last 4 a long time given that Fujishima and Honda's first file of sun-assisted water splitting on titanic [1]. As a end result of techno-monetary calculation [2], constant-mattress photo catalytic reactor [3,4] and hydride photo electrodes [5,6] have been crowned as the only systems for solar-assisted hydrogen production, partially because of the fact that both designs might depend upon

different present technologies, i.e. Environmental remediation [7,8] and multi-junction solar cells [9], respectively. To be actually economically feasible, it's far vital to expand photocatalysts that have match- in a position microelectronic residences for efficient water splitting, are less expensive to manufacture and corrosion-resistant. To date, no single recognised semiconductor material satisfies all aforementioned standards and in depth research remains being performed to pick out the cloth training that could permit for massive-scale commercialization of solar-assisted water cutting generation. Titanium dioxide and tungsten trioxide have been taken into consideration very promising water splitting structures because the early ages of PEC research, specifically due to their low-cost, proper electric conductivity and resistance to corrosion. However, their highly large optical band hole energies (EG, TiO_2 $\frac{1}{4}$ 3.2 eV [1], EG, WO_3 $\frac{1}{4}$ 2.6 eV [10]) severely restriction their absorption of the sun spectrum, leading to maximum sun-to-hydrogen efficiencies of ca. three% [11,12] simplest. The reduction of transition metal oxide band gaps has been the Holy GRAIL of PEC research in the beyond decade And many tries have been stated, typically thru incorporation of overseas elements [13,14,15]. Unfortunately, metal oxide band hole discount is normally observed via a lower in PEC performances [16], as the desired overseas element concentration (at the least four percentage in WO_3 [15]) leads in maximum cases to malign micro structural defects [16, 17]. In contrast with the latter steel oxides, hematite ($\alpha\text{-Fe}_2\text{O}_3$) is a material magnificence that inherently has properly matched absorption traits for solar-powered water splitting. Indeed, its band gap (2.0e2.2 eV [18]) is considered perfect since it permits an most effective balance between photo present day density (assuming one hundred% photo-conversion above band gap) and generated picture-voltage [19]. However, hematite falls short on electric performances, with hollow-diffusion duration in the order of 20 nm [20], although big progress in Fe_2O_3 nano-structuring has been made to cope with this trouble [21, 22]. With an digital band gap of 2.2e2.3 eV and better positioned valence band maximum for water splitting than all the aforementioned metal oxide systems [23, 24,25], copper tungsten (CuWO_4) is a promising fabric-elegance that deserves further research. To the best of our information, much less than ten papers have been posted in particular on the picture- electrochemical residences of CuWO_4 due to the fact that Benko's first file in 1982 [26]. These initial consequences were acquired on Poly crystalline samples synthesized by using solid-state reaction approach. Attempts to reduce CuWO_4 bulk resistivity with indium oxide had been stated by way of the authors and large image-pastime beneath xenon arc lamp illumination turned into located in Na_2HPO_4 solution (pH9). The subsequent examine posted in 1984 with the aid of Dourer on mono crystalline samples confirmed the conductivity to be n-type [27], with a donor attention of $5.5 \times 10^{19} \text{ cm}^{-3}$. MotteSchottky analyses made in 1990 by means of Arora on single crystals revealed a flat-band capability for copper tungstate (-0.48 VSCE in pH1.5 answer, -0.15 VRHE) that would even permit for unbiased water splitting [24]. The first skinny film CuWO_4 photo electrode fabrication became stated in 2005 by way of Pandey using spray-deposition technique [28]. Resulting copper tungstate samples examined in a photo- voltaic electrochemical mobile configuration with $\text{Ce}^{4+}/\text{Ce}^{3+}$ redox couple exhibited a brief-circuit cutting-edge (now not normalized to vicinity), an open circuit ability and an efficiency of 0.3 mA, and 0.sixty four%, respectively. In an try and reduce CuWO_4 optical band hole, Chen evolved a low-temperature co-sputtering technique to synthesize amorphous $\text{Cu}_x\text{W}_{(1-x)}\text{O}_4$ thin movies [29]. Although copper

2. Experimental methods

2.1. CuWO_4 -based photo electrode preparation

$\text{CuWO}_4/\text{eMWCNT}$ nanocomposites thin films had been fabricated by using spray pyrolysis method. Two answers, one for Cu and W precursors and one for MWCNT, have been initially organized then combined collectively. The resultant solution become then sprayed down onto a hot plate containing the substrates. All chemicals have been used as acquired from industrial assets. The solution containing equimolar copper and tungsten chemical precursors (generally 10 mM) become acquired by dissolving copper acetate ($\text{Cu}(\text{ac})$, 99.94%, J. T. Baker Chemical Co.) and ammonium metatungstate (AMT, 99.99%, Inflamed Advanced Materials) in

double-distilled water (18 MU.Cm). The acquired answer changed into ultrasonic for 10 min to reap entire dissolution of chemical precursors and make certain composition homogeneity. For the second answer, multi-wall carbon nanotubes (Diam. \times L : 20e30 nm \times 2e4 mm, electric conductivity w100 S cm⁻¹, Cheap tubes Inc.) were dispersed in double-distilled water the usage of either a low-strength ultrasonic system (NEY Ultrasonic 57X, Lab Extreme Inc.) or a 100W 20 kHz stainless-steel horn (Vibrant Cell, Sonics & Materials, Inc.) dipped at once into the solution. Solutions containing copper/tungsten precursors and MWCNT were then blended to attain the favoured MWCNT: CuWO₄ weight ratio (see Result segment for information). The resulting answer become sprayed the use of an airbrush (Paasche, siphon feed single movement) onto SnO₂:F-covered glass substrates (TEC 15, Hartford Glass) cleaned in a soap/DI-water/acetone/DI-water/methanol/ DI-water/isopropanol sequence. The airbrush-sample distance turned into set to twenty cm to ensure uniform coating. During the deposition, MWCNT-Cu (ac)/AMT combos had been continuously stirred to warrant uniform distribution of the multi-wall carbon nanotubes within the final sprayed CuWO₄ skinny films. The deposition temperature, spray fee, and air static pressure were set at 275 °C, 1 mL min⁻¹ and 35 psi, respectively. These parameters had been found to be gold standard to produce thin movies with thickness version less than eight% across 25 \times 25 mm²

2.2. Material characterization

Films thicknesses (usually 2.0 \pm 0.1 mm) had been measured by profilometer the usage of a Tencor Alpha Step 200 profilometer. The surface morphology of the samples becomes characterized with a Hitachi S-4800 scanning electron microscope (SEM) at an acceleration voltage of 20 kV. Elemental composition changed into determined by using power-dispersive X-ray spectroscopy (EDS) the usage of an Oxford INCA Energy 250 \times 3 with INCA PentaFETx-3 Si Li detector. Nanocomposites structures were photographed on a Hitachi HT7700 transmission electron microscope (TEM) operating at 100 KV with an AMT XR41 four megapixel dig cam (Advanced Microscopy Techniques, Corp.). In order to samples. As-deposited samples wherein eventually submit-annealed in air until crystallization turned into achieved (see Result section for details). determine the temperature at which CuWO₄ crystallization happens, X-ray diffractograms were recorded in situ under 1 atm air stress at temperatures starting from deposition temperature 275 °C to 550 °C in steps of fifty °C, at the Wiggler Insertion Device Experimental Station 7-2 at Stanford Synchrotron Radiation Light source (SLAC). The X-ray power changed into monochromatic with a Si (111) crystal to 10,150 eV, corresponding to a wavelength of 0.12229 nm. Data acquisition was executed with the SPEC software package deal. The herein investigated pattern changed into an (MWCNT-unfastened) as-deposited CuWO₄ film, which turned into constant at the diffract meter degree in a polyimide case and in contact with a thermo couple. Optical homes of sintered CuWO₄ and CuWO₄-MWCNT composite (later referred as nanocomposites) movies had been measured with a Lambda 2 Perkins Elmer spectrophotometer between 350 and 1100 nm.

2.3. Photo electrochemical measurements

Electrochemical analyses had been finished with a Gamry 600 potentiostatic. The take a look at mobile consisted of CuWO₄-primarily based PEC electrode (usually 2 cm²), a platinum foil counter electrode (10 cm²) and saturated calomel reference electrode. Hydroid pH10 buffer solutions (0.25M sodium bicarbonate/0.25M sodium carbonate, conductivity $\frac{1}{4}$ 11 mS cm⁻¹) had been used for all assessments provided within the gift manuscript (see Results and Discussion segment concerning pH choice). Photo electrodes were irradiated with simulated AM1.5G illumination provided by an Oriel elegance A sun simulator prepared with Newport 1000W xenon arc lamp and AM1.5G filter. The simulator changed into calibrated the usage of an International Light Technologies 900 spectrometer such that its irradiance corresponded to that of AM1.5G in the absorption variety of CuWO₄ (i.e. 280 W.M⁻² from 250 nm to 560 nm, Figure S1). The impact of MWCNT on photo anodes conductivity became assessed by way of electrochemical impedance spectroscopy (EIS) at 0.8 VSCE in pH10 buffer answer (1.63 VRHE) with frequencies starting from 1 Hz to at least one MHz Linear sweep voltammetry (LSV) scans had been

measured in a 3-electrode configuration at a price of 25 mV s⁻¹. Finally, incident photon-to-electron efficiency (IPCE) and photocurrent spectroscopy (PS) measurements were obtained using a PVmeas QE7 system.

3. Results and discussion

3.1. Physical properties of un-modified CuWO₄ thin films

As evidenced in our previous communiqué on reactively co-sputtered copper tungsten [23], sintering situations are decisive to gain photo energetic CuWO₄ anodes. In order to determine greatest pyrolysis of sprayed samples, a collection of X-ray diffractograms had been taken at SLAC on an as-deposited (substrate temperature: 275 °C) stoichiometric ([W]/[Cu] $\frac{1}{4}$ 1.03) CuWO₄ sample placed on a dedicated annealing level and heated from 3-50 °C to 550 °C, in temperature steps of 50 °C. At every temperature step, a plateau of 30 min became held before the diffractogram changed into acquired. The results of this evaluation provided in Fig. 1 suggest that

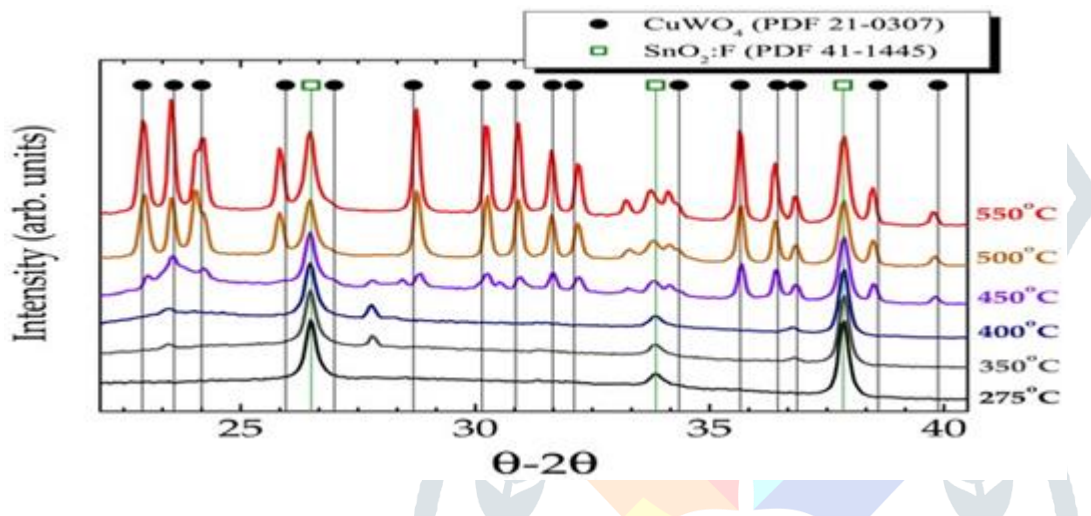


Fig. 1 e X-ray diffractograms of as-deposited CuWO₄ thin movie recorded in-situ in air at temperatures from 275 °C to 550 °C. Each temperature step became held for 30 min earlier than X-ray diffractogram become taken. The X-ray power became 10,150 eV. These peaks had been related to mono clinic tungsten trioxide (PDF 43e1035), suggesting that spray-deposited CuWO₄ skinny films annealed as much as 550 °C include a small fraction of tungsten trioxide inside. It need to be stated that comparable WO₃ diffraction capabilities had been determined on reactively co-sputtered CuWO₄ thin films after annealing in Ar at 500 °C [23], even though the W-to-Cu ratio had been determined to be near harmony (1.05, as measured by EDS). Subsequent evaluation indicated that A temperature of at least 800 °C changed into vital to reap a natural CuWO₄ segment, as indicated in Figure S2 through the XRD pattern measured on a CuWO₄ thin movie sprayed (referred as SP-800) on a (100) silicon wafer and annealed in air for five h at this temperature. The morphology of spray-deposited CuWO₄ thin movie after annealing is provided in Fig. 2. At low magnification (Fig. 2a), the floor of the movie appears pretty uniform (i.e. No solvent drop lines) and crack-loose. A closer look well-known shows that spray-deposited CuWO₄ is basically a porous material (Fig. 2b and c), fabricated from micrometer length aggregates spaced by means of pores with length in the 200e500 nm variety. Such architecture should permit electrolyte to permeate the CuWO₄ shape, a capacity nice feature for PEC and electro chromic programs [32]. Higher magnification photographs (Fig. 2d) indicate that aggregates had been produced from CuWO₄ nanoparticles, the diameters of which ranged from 20 to 50 nm. Subsequent UV-visible spectroscopy evaluation become accomplished on brownish annealed CuWO₄ skinny films to decide their optical characteristics. Transmittance and reflectance spectra had been then

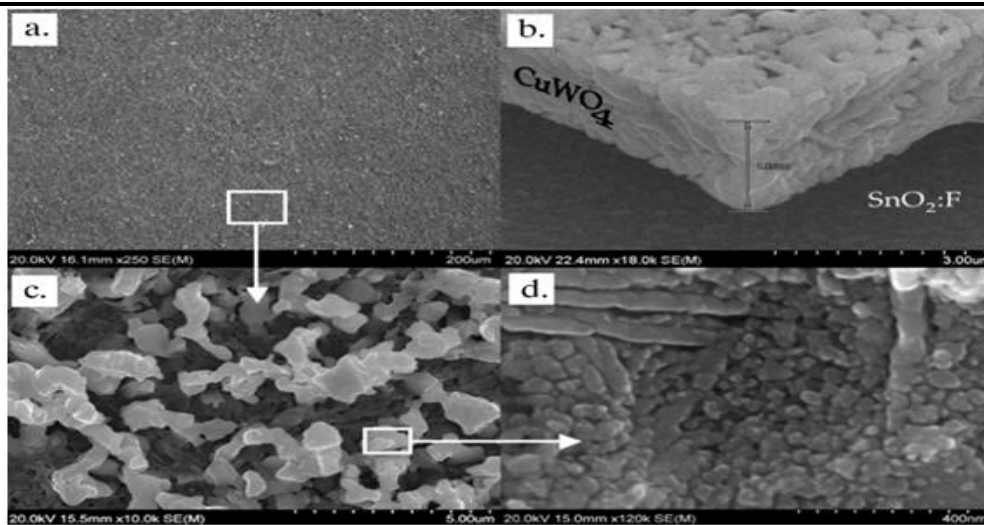


Fig. 2 e Top- and bird's-eye views micrographs obtained by scanning electron microscopy on spray-deposited CuWO_4 thin films after annealing at 500°C for 2 h. This observation indicates that the resulting thin films were (a) crack-free, (b, c) porous and (d) made of CuWO_4 nanoparticles which sizes ranged from 20 to 50 nm. used to assemble the Tauc plot, assuming allowed indirect optical transition [26]. As presented in Fig. three, spray-deposited CuWO_4 skinny films owned an indirect band gap of two.25 (T0.05) eV, a standard value previously suggested for this material elegance [23,33]. This became accompanied up by photocurrent spectroscopy analysis to make sure that fee providers might be effectively generated and accumulated at photon power equal or larger than 2.25 eV. This check becomes achieved under monochromatic mild from 350 nm to 650 nm in pH10 buffer answer at 0.8 VSCE (1.63 VRHE). As supplied within the inset of Fig.3, a band hole of 2.21 (T0.05) eV become acquired from this analysis, a fee analogous to the one acquired by means of optical methods. Based on those measurements, the theoretical photo present day density limit for copper tungstate cloth class turned into defined as 10.7 mA cm^{-2} , a cost that would normally permit for a solar-to-hydrogen performance of 13% (assuming 100% Faradic efficiency).

3.2. Photo electrochemical properties of un-modified CuWO_4

Photo electrochemical characterizations have been completed to assess the water-splitting ability of spray-deposited CuWO_4 thin movies. A MotteSchottky plot obtained on this cloth in pH10 buffer answer under AM1.5G simulated illumination is supplied within the inset of Fig. 4. It was discovered that annealed CuWO_4 fabric exhibited n-type conductivity and possessed a fee carrier density of $2.6 \times 10^{18} \text{ cm}^{-3}$ (using a dielectric constant of 83 for CuWO_4 [34] and an effective mass for electron of 70 [27]), a fee comparable with different said on unmarried crystal copper tungsten [24]. Extrapolating the MotteSchottky curve to at least $1/C^2 \frac{1}{4} 0$ caused a flat-band potential (VFB) of -0.1 VSCE (0.73 VRHE), a cost later confirmed by means of illuminated open circuit ability beneath a 5-sun simulated illumination (Figure S3, pinnacle) and LSV test, the use of the capacity at which the present day regime transfer from anodize to cathodic (Figure S3, backside). This flat-band capacity differs appreciably from values previously pronounced for poly crystalline

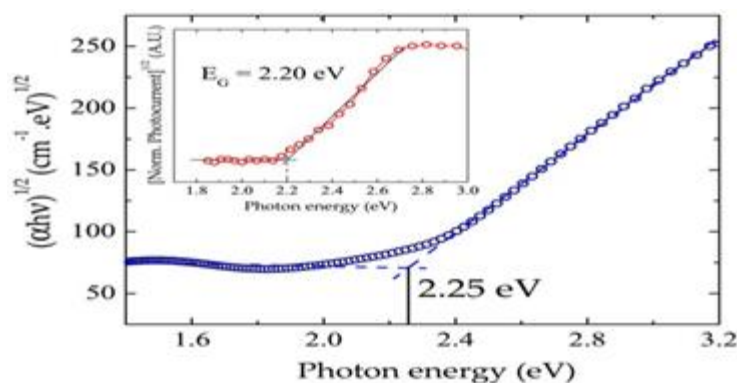
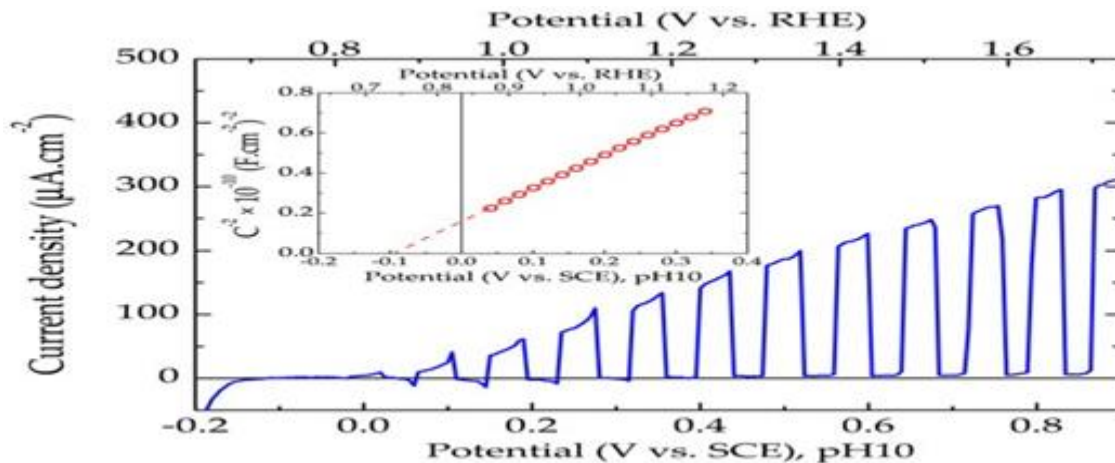


Fig.3e Tauc plots of annealed CuWO₄ thin film material derived from both UV-visible and (Inset) photocurrent spectroscopy (PS) spectra. PS data were measured 0.8 V_{SCE} in pH10 buffer solution (1.63 V_{RHE}). Both methods led to consistent band gap values (2.20 ± 0.05 eV).

Fig. 4 e Linear sweep voltammetry of annealed CuWO₄ photo anodes measured in a three-electrode configuration in pH10 buffer answer under chopped simulated AM1.5G illumination (test price: 25 mV sL1). (Inset) MotteSchottky plot measured on annealed CuWO₄ in pH 10 buffer answers under AM1.5G



Illumination. CuWO₄ systems received through physical deposition strategies (co-sputtering: VFB $\frac{1}{4}$ —0.03 VRHE [23]; solid-kingdom response: VFB $\frac{1}{4}$ —0.15 VRHE [24]) and examined in acidic media. Supplementary MotteSchottky (M — S) analyses were performed in pH10, 9, 8, 6.86, 5, 3 and a couple of buffer answers on a representative CuWO₄ spray-deposited pattern to understand the foundation of such anodic shift of VFB. As shown in Figure S4, the MeS curves measured in unique pHs on the identical pattern vary most effective from the Flat-band potential values, which pH dependency follows fairly nicely the Nernst equation (C.A. —50 mV/ pH). This might indicate that floor Fermi stage pinning won't be the main cause for the VFB anodic shift measured on spray-deposited CuWO₄ in pH10 when as compared to those mentioned in acidic solution, despite the fact that extra flat-band measurements in non aqueous answers with regarded Redox species could be vital to rule out the feasible impact of prolongation/deprotonation on CuWO₄ surface polarization. However, a solid photograph modern density was discovered underneath potentiostatic situations (0.8 VSCE, 1.sixty three VRHE) in Hydrion pH10 buffer solution for as much as 24 h to date tested (Figure S6), justifying using this electrolyte inside the present record.

The difference inside the microstructure and crystallographic structure, as a long way as discernible with X-ray diffraction, between CuWO₄ substances received by bodily methods (co-sputtering [23] or stable-state response [24]) and spray deposition (this report) pointed us to a rational for the located variations inside the anodic shift of the flat-band potential. Figure S2 affords the X-ray diffract grams received on CuWO₄ synthesized via spray pyrolysis after a publish-deposition annealing in air at 500 °C (henceforth SP-500) and 800 °C (henceforth SP-800) as compared to the only obtained on co-sputtered skinny film after a 500 °C annealing in Ar [23] (henceforth PVD-500). It seems that the PVD-500 and SP-800 samples have a pretty comparable micro shape (the WO₃ section aside), as far as the preferential orientation in their 111 crystal planes is involved. However, the diffract gram acquired on SP-500 differed pretty and coffee (i.E. 110 and 111) Miller indices have been recorded with comparable intensities. The impact of crystallographic orientation on cloth floor lively characteristics is a famous phenomenon that has been experimentally established at both macroscopic [35] and microscopic [36] scales. This phenomenon is defined by using floor dipole strength modulation arising from numerous surface atomic densities, reconstructions and chemistries taking place at each crystallographic side [37]. The floor band diagram of

spray-deposited CuWO_4 derived from EIS and UV-visible spectroscopy analyses is offered in Fig. 5. For the sake of assessment,

Fig.5e Surface band diagram of CuWO_4 and WO_3 materials synthesized by spray pyrolysis technique. Identical tungsten chemical precursor (ammonium metatungstate) was used in the formulation of both films.

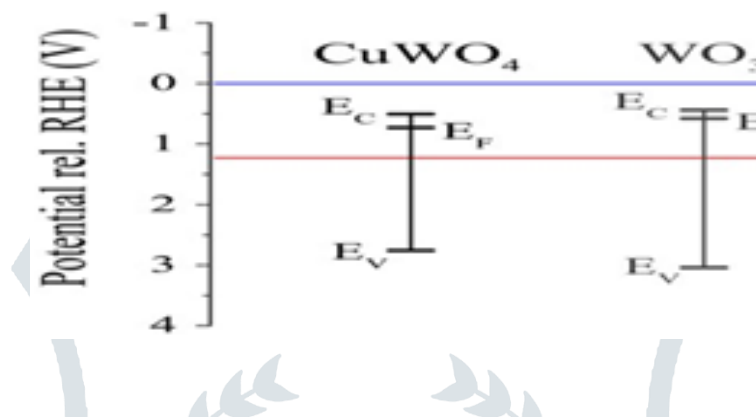


Diagram of WO_3 (obtained additionally by spray pyrolysis the usage of the equal tungsten precursor used inside the fabrication of CuWO_4 , i.e. AMT, and annealed for two h at 500°C in air) is also presented. Here, a dielectric permitting of 50 and an effective mass for electrons of 2.42 had been used for the willpower of the donor density of tungsten oxide ($N_D \frac{1}{4} 2.6 \times 10^{18} \text{ cm}^{-3}$). This evaluation indicates that the position of CBM stays pretty un- changed among CuWO_4 and WO_3 , while VBM in CuWO_4 is placed four hundred mV closer to OER than it is in WO_3 , in top agreement with current findings [30]. Fig. 4 offers an ordinary linear test voltammogram obtained underneath chopped AM1.5G simulated illumination on a sprig-deposited CuWO_4 skinny movie in pH10 buffer solution. Here, a clean reaction to chopped mild is found from $-50 \text{ mV}_{\text{SCE}}$ (0.78 VRHE), with a most photograph modern-day density of approximately 300 mA cm^{-2} at 0.8 VSCE (1.63 VRHE). Beyond this factor, huge darkish contemporary ($>20 \text{ mA cm}^{-2}$) become determined and LSV scans had been stopped. It should be mentioned that considerable anodic and cathodic modern transients had been located at the chopped LSV function for capacity decrease than c.A. 0.30 VSCE (1.13 VRHE). The anodic current transients found upon illumination characterizes photograph- generated holes gathered close to the CuWO_4 /electrolyte interface that don't contribute to the oxygen evolution re- action, while cathodic modern transients discovered while mild became grew to become off corresponds to the recombination of accumulated holes with electrons from the conduction band.

Hydrogen peroxide become subsequently delivered as a hole scavenger to the pH10 buffer answer in an effort to mitigate the injection barrier observed in low capacity regime. Fig. 6 gives the photocurrent density (corrected for dark cur lease) measured as characteristic of potential before and after addition of 5 mm H_2O_2 . A clean photocurrent density increase at potentials lower than 0.30 VSCE (1.13 VRHE) befell after addition of

H₂O₂. This suggests that the

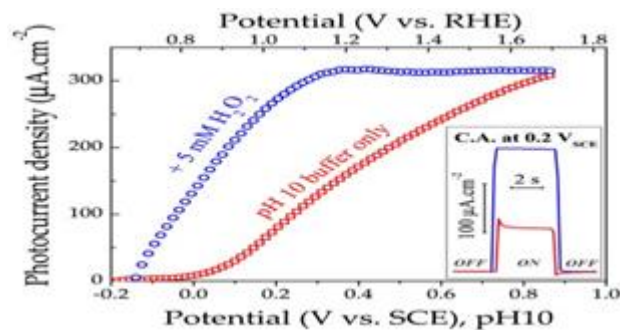
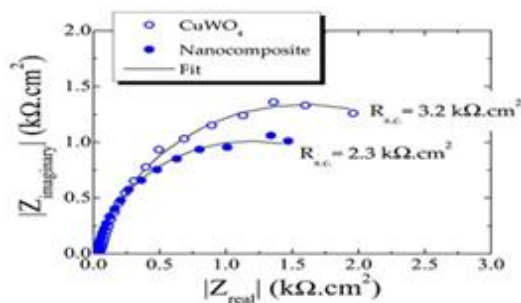


Fig. 6 e Photocurrent density as feature of applied ability characteristics measured on CuWO₄ photograph anodes under simulated AM1.5G illumination in pH10 buffer solution before (open pink squares) and after (open blue circles) addition of H₂O₂. CuWO₄/electrolyte interface but injected into the solution, taking part to hydrogen peroxide dissociation response. This locating became additionally confirmed by way of chronometer analyses accomplished at zero.2 VSCE (1.03 VRHE) on CuWO₄ image- anodes underneath chopped simulated AM1.5G illumination before and after the addition of hydrogen peroxide. As provided in the inset in Fig. 6, both anodic and cathodic modern-day transients have been suppressed after addition of the hole scavenger. For ability more than 0.30 VSCE (1.13 VRHE), a constant photo- modern density become observed on LSV characteristics after addition of hydrogen peroxide, accomplished regardless of the hole injection yield at the CuWO₄/electrolyte interface (i.e. without or with hole scavenger), represents best a thirty-5th of the theoretical image present day density a 2.2 eV band hole cloth should generate (10.7 mA cm⁻²). Therefore, bad bulk transport homes were taken into consideration as the most possibly

3.3 Physical properties of nanocomposites

The use of CNT as fee collector in PEC structures or dye-sensitized solar cells isn't always a unique concept and effects on devices performance development with CNT have been said on numerous light absorber nano systems, along with Fe₂O₃ [45], TiO₂ [46,47] and ZnO [48]. So some distance, most important techniques have been used to synthesize those structures: (i) simultaneous deposition of the solar absorber and CNT over a obvious conductive oxide (TCO) substrate, each being blended previous the synthesis, or (ii) deposition of the sun absorber over a bed of CNT. Though especially powerful in improving photo generated fee collection, technique (ii) won't be like minded with PEC/PV (hybrid) systems, because the compact layer formed by CNT networks would doubtlessly decrease photons transmission with power underneath the band gap of the top-lying PEC thin film to the underlying sun mobile(s). Thus, we postulate that technique (i) should be a more powerful technique, as the quantity of CNT integrated into the sun absorber bulk matrix can be refined such that it leads to an appropriate stability among electric and optical residences. The effectiveness of the existing mild ABSORBER/CHARGE collector composite method relies frequently on the capacity to gain a picture electrode thin movie wherein MWCNTs are uniformly dispensed at some point of. Considering the spray solution education method defined within the experimental segment, the MWCNT must be well dispersed in double-distilled water before being brought them to the answer containing the copper and tungsten chemical precursors. Two apparatuses had been examined to disperse MWCNT in answer: a low-power ultrasonic system and a 100W 20 kHz stainless-steel tip dipped without delay.

4. Photo electrochemical performances of nanocomposites.

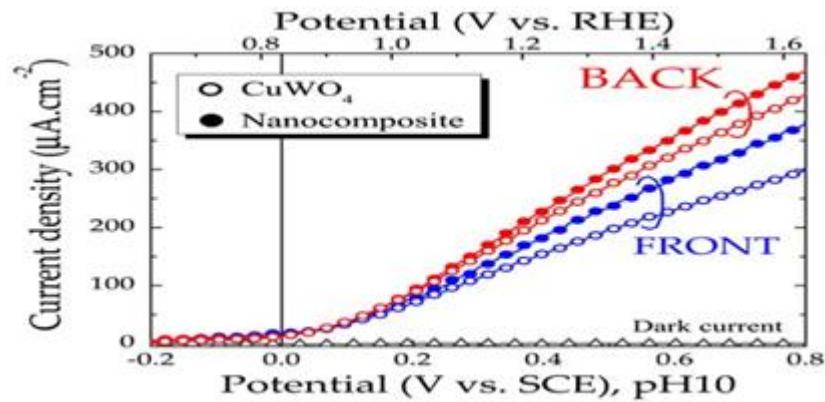


Electrochemical impedance spectroscopy analyses were performed to assess the effect of MWCNT on the electronic

Fig. 8 e Nyquist plots of CuWO_4 (open symbols) and nanocomposites photo anodes (closed symbols) measured at $0.8 V_{\text{SCE}}$ in pH10 buffer solution ($1.63 V_{\text{RHE}}$) under simulated AM1.5G illumination (AC voltage :)

The Nyquist plots obtained on nanocomposites and un-modified CuWO_4 photo- anodes at $0.8 V_{\text{SCE}}$ in pH10 buffer solution ($1.63 V_{\text{RHE}}$) under simulated AM1.5G

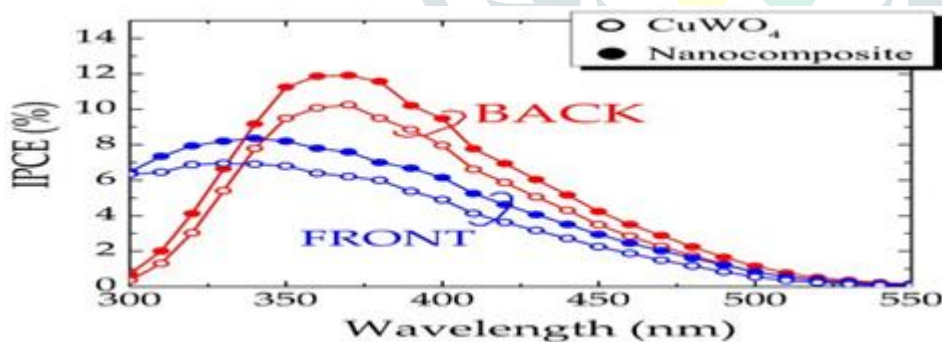
Illumination is presented in Fig. eight. Experimental statistics were fitted with an equivalent circuit containing the semiconductor bulk resistance $R_{s.c}$. In parallel with a regular phase element (CPE), related to a series resistance R_s [R_s —($R_{s.c}$ //CPE)]. For un-modified CuWO_4 thin movies, a bulk resistance of 3200 U cm^2 was measured. However, the bulk resistance changed into decreased with the addition of MWCNT down to 2300 U cm^2 , corresponding to a reduction in resistance of about 30%. These effects confirmed the benefit of carbon annotates on photo electrodes transport houses formerly reported on other steel oxide systems [45,46,47,48], justifying their use in the light absorber/charge collector composite approach.. In reality, it turned into discovered by using UV-visible spectroscopy (records no longer proven) that optimized MWCNT: CuWO_4 nanocomposites systems experienced a loss in transmittance much less than 2% when compared to un-changed CuWO_4 .



The LSV scans measured on un-modified CuWO₄ and nanocomposites samples under the front-side or lower back-aspect simulated AM1.5G illumination is provided in Fig. 9. The absorption of the SnO₂:F/glass substrates became now not taken into account within the calibration of the solar simulator for lower back-facet

Fig. 9 e Linear sweep voltammeter of CuWO₄ (open symbols) and nanocomposites (closed symbols) photo anodes measured in a three-electrode configuration in pH10 buffer answer underneath the front-facet (blue symbols) and returned-aspect (red symbols) simulated AM1.5G illumination.

Finally, incident photon-to-contemporary spectroscopy (IPCE) analyses had been finished on both un-changed CuWO₄ and nanocomposites photograph anodes at a capability of 0.8 VSCE in pH10 buffer answer (1.63 V RHE) below the front-facet and returned-aspect monochromatic illumination (Fig. 10). Note that experimental data acquired underneath lower back-side illumination have been not corrected for the absorption of SnO₂:F/glass substrates. The fashion in PEC performances determined by using LSV analyses inside the high capability regime became confirmed by way of IPCE measurements, i.e. Photon-to-modern-day efficiencies had been more below returned-facet illumination for both systems while nanocomposites exhibited maximum efficiencies over un-changed CuWO₄ photograph anodes irrespective



This observe tested that a mild absorber/charge collector composite technique should be used to enhance the performances of image electrochemical systems regarded to be limited through poor price transport properties. In the gift take a look at, the usage of conductive MWCNT successfully reduced the bulk resistance of spray-deposited CuWO₄ skinny films by way of 30%, permitting for a most image modern density of almost 0.5 mA cm⁻² below back-side illumination

5. Conclusions

We mentioned in this communication on a mild Absorber/charge collector composite approach to improve the image- electrochemical performances of CuWO₄ fabric elegance. A spray deposition system become in particular developed the use of copper acetate and ammonium metatungstate as chemical precursors for copper and tungsten,

respectively. A publish- annealing step in air at 500 °C for 2 h changed into required to attain CuWO₄ crystallographic section. Resulting copper tungstate samples had been porous, but crack-free, and made of CuWO₄ nano debris with dimensions in the 20e50 nm range. Tauc plots derived from UV-Vis and photo modern spectroscopy techniques led basically to regular band gap values of 2.20 (T_{0.05}) eV. With such optical traits, A sun-to-hydrogen efficiency of 13% will be completed, assuming total absorption and conversion of photons with strength above band hole and 100% Faradic performance. Electrically conductive MWCNT have been then added to the copper and tungsten chemical precursors to shape CuWO₄/MWCNT nanocomposites image electrodes. TEM analysis discovered that CuWO₄ nano debris had been firmly anchored to the carbon nanotubes an essential feature in the mild Absorbed/fee collector composite approach. Electrochemical impedance spectroscopy analyses pointed out that a MWCNT: CuWO₄ weight ratio of 1:10,000 ought to decrease the bulk resistance from 3200 Ω cm² to 2300 Ω cm² without appreciably changing the picture anode optical residences. Subsequent linear scan voltammetry scans done underneath front-side illumination revealed a photo present day density increase of 26% inside the excessive ability regime with addition of MWCNT, in appropriate agreement with the 30% discount in bulk resistance found by EIS. A hollow injection barrier turned into diagnosed as the main foundation for modest CuWO₄ PEC performances in

References

- [1] Fujishima A, Honda K. Electrochemical photolysis of water at a semiconductor electrode. *Nature* 1972;238:37e8.
- [2] James BD, Baum GN, Perez J, Baum KN. Technoeconomic analysis of photoelectrochemical (PEC) hydrogen production. Directed Technologies, Inc, https://www1.eere.energy.gov/hydrogenandfuelcells/pdfs/pec_technoeconomic_analysis.pdf; 2009.
- [3] Braham RJ, Harris AT. Review of major design and scale-up considerations for solar photocatalytic reactors. *Ind Eng Chem Res* 2009;48:8890e905.
- [4] Zou Z, Ye J, Sayama K, Arakawa H. Direct splitting of water under visible light irradiation with an oxide semiconductor photocatalyst. *Nature* 2001;414:625e7.
- [5] Miller E, Marsen B, Paluselli D, Rocheleau R. Optimization of hybrid photoelectrodes for solar water-splitting. *Electrochemical Solid-state Lett* 2005;8:A247e9.
- [6] Khaselev OK, Turner JA. A monolithic photovoltaic- photoelectrochemical device for hydrogen production via water splitting. *Science* 1998;280:425e7.
- [7] McCullagh C, Skillen N, Adams M, Robertson P. Photocatalytic reactors for environmental remediation: a review. *J Chem Technol Biotechnol* 2011;86:1002e17.
- [8] Chong MN, Jin B, Chow CW, Saint C. Recent developments in photocatalytic water treatment technology: a review. *Water Res* 2010;44:2997e3027.
- [9] King RR, Fetzer CM, Colter PC, Edmondson KM, Ermer JH, Cotal HL, et al. High-efficiency space and terrestrial multijunction solar cells through bandgap control in cell structures. *PVSC* 2002:776e81.
- [10] Gaillard N, Cole B, Kaneshiro J, Miller EL, Marsen B, Weinhardt L, et al. Improved current collection in WO₃:Mo/WO₃ bilayer photoelectrodes. *J Mater Res* 2010;25: 45e51.
- [11] Gaillard N, Chang Y, Kaneshiro J, Deangelis A, Miller EL. Status of research on tungsten oxide-based photoelectrochemical devices at the university of hawaii. In: *Solar Hydrogen and Nanotechnology V.*, vol. 7770. Proc. SPIE; 2010. 77700Ve14.
- [12] Lee WJ, Shinde PS, Go GH, Ramasamy E. Ag grid induced photocurrent enhancement in WO₃ photoanodes and their scale-up performance toward photoelectrochemical H₂ generation. *Int J Hydrogen* 2011;36:5262e70.

- [13] Asahi R, Morikawa T, Ohwaki T, Aoki K, Taga Y. Visible-light photocatalysis in nitrogen-doped titanium oxides. *Science* 2001;293:269e71.
- [14] Morikawa T, Asahi R, Ohwaki T, Aoki K, Taga Y. Band-gap narrowing of titanium dioxide by nitrogen doping. *J J Appl Phys* 2001;40:561e3.
- [15] Huda MN, Yan Y, Moon C, Wei S, Jassim MM. Density- functional theory study of the effects of atomic impurity on the band edges of monoclinic WO_3 . *Phys Rev B* 2008;77: 195102e14.
- [16] Cole B, Marsen B, Miller EL, Yan Y, To B, Jones K, et al. Evaluation of nitrogen doping of tungsten oxide for photoelectrochemical water splitting. *J Phys Chem C* 2008; 112:5213e20.
- [17] D'Arienzo M, Siedl N, Sternig A, Scotti R, Morazzoni F, Bernardi J, et al. Solar light and dopant-induced.
- [18] Hardee KL, Bard AJ. Semiconductor electrodes. X. photoelectrochemical behavior of several polycrystalline metal oxide electrodes in aqueous solutions. *J Electrochem Soc* 1977;124:215.
- [19] Chen Z, Jaramillo TF, Deutsch TG, Shwarscstein AK, Forman AJ, Gaillard N, et al. Accelerating materials development for photoelectrochemical hydrogen production: standards for methods, definitions, and reporting protocols. *J Mater Res* 2010;25:3e16.
- [20] Dare-edwards MP, Goodenough JB, Hamnett A, Trevellick PR. Electrochemistry and photoelectrochemistry of iron(III) oxide. *J Chem Soc Faraday Trans* 1983;79:2027e41.
- [21] Sivula K, Formal FL, Gratzel M. Solar water splitting: progress using hematite ($\alpha\text{-Fe}_2\text{O}_3$) photoelectrodes. *ChemSusChem* 2011;18:432e49.
- [22] Vayssieres L, Sathe C, Butorin S, Shuh D, Nordgren J, Guo J. One-dimensional quantum-confinement effect $\alpha\text{-Fe}_2\text{O}_3$ ultrafine nanorod arrays. *Adv Mater* 2005;17:2320e3.
- [23] Chang Y, Braun A, Deangelis A, Kaneshiro J, Gaillard N. Effect of thermal treatment on the crystallographic surface energetics and photoelectrochemical properties of reactively cosputtered copper tungstate for water splitting. *J Phys Chem C* 2011;115:25490e5.
- [24] Arora SK, Mathew T, Batra NM. Electrochemical characteristics of copper tungstate single crystals. *J Phys D Appl Phys* 1990;23:460e4.
- [25] Chen S, Wang L. Thermodynamic Oxidation and Reduction Potentials of Photocatalytic Semiconductors in Aqueous Solution. arXiv:1203.1970v1 [cond-mat.mtrl-sci]: 2012.
- [26] Benko FA, MacLaurin CL, Koffyberg FP. CuWO_4 and Cu_3WO_6 as anodes for the photoelectrolysis of water. *Mat Res Bull* 1982;17:133e6.
- [27] Doumerc JP, Hejtmanek J, Chaminade JP, Pouchard M, Krussanova M. A photoelectrochemical study of CuWO_4 single crystals. *Phys Stat Sol A* 1984;82:285e94.
- [28] Pandey PK, Bhave NS, Kharat RB. Spray deposition process of polycrystalline thin films of CuWO_4 and study on its photovoltaic electrochemical properties. *Mater Lett* 2005;59: 3149e55.
- [29] Chen L, Shet S, Tang H, Ahn K, Wang H, Yan Y, et al. Amorphous copper tungsten oxide with tunable abnd gaps. *J Appl Phys* 2010;108:043502 1e043502 5.
- [30] Yourey JE, Bartlett BM. Electrochemical deposition and photoelectrochemistry of CuWO_4 , a promising photoanode for water oxidation. *J Mater Chem* 2011;21:7651e60.